Available online at www.sciencedirect.com
SCIENCE DIRECT®
International Journal of Thermal Sciences 43 (2004) 1125–1139
International Journal of Thermal Sciences
www.elsevier.com/locate/ijts

Towards a unifying heat transfer correlation for the entire boiling curve

Torsten Lüttich [a], Wolfgang Marquardt [a,*], Martin Buchholz [b], Hein Auracher [b]

[a] *Lehrstuhl für Prozesstechnik, RWTH Aachen, 52064 Aachen, Germany*
[b] *Institut für Energietechnik, TU-Berlin, 10587 Berlin, Germany*

Received 16 December 2003; received in revised form 23 April 2004; accepted 23 April 2004

Available online 20 July 2004

Abstract

The mechanistic understanding of boiling processes is still inadequate. Major physical effects determining the heat transfer in high heat flux nucleate and transition boiling regions have not yet been captured adequately. Thus, existing design correlations are often valid only for one of the boiling regimes. In this paper, the wetting structure close to the boiling surface is identified using the experimental data from an optical probe, obtained during pool boiling of FC-72 on a horizontal surface, together with a mathematical model for the interfacial geometry based on two-phase flow averaging theory. In the same framework, a unifying correlation to describe the heat flux along the entire boiling curve is presented. The suggested correlation is based on the same physical quantities regardless of the boiling regime; it employs only a single fitting parameter in its most simple form. Alternative correlations are compared to the suggested correlation and their relative merit is assessed by statistical model discrimination techniques. The results suggest that transfer phenomena associated with the interfacial evolution, in particular the volumetric presence of interface close to the heater surface, together with the superheat, play an important role for the overall boiling heat transfer mechanism.

PACS: 44.20.+b; 44.35.+c; 68.03.Fg; 68.03.Hj

Keywords: Boiling; Multi-phase flow averaging theory; Identification; Interfacial area density; Contact angle; Wetting; Microlayer theory

1. Introduction

In the last decades many experimental and theoretical investigations on boiling heat transfer have been conducted. Despite all the efforts, relevant physical parameters, which allow a *unifying description of the entire boiling curve*, have not been identified. Existing design correlations are often valid only for one of the boiling regimes, i.e., nucleate boiling, critical heat flux, transition and film boiling. Their uncertainty is partly rather large, especially for higher heat fluxes, where a mechanistic understanding of the boiling process is still inadequate. Depending on the boiling regime, the heat flux to the boiling fluid has been correlated with different quantities [1]. Among the most prominent are superheat, nucleation site density, average vapor fraction at the boiling surface or average vapor velocity, but there are many others such as bubble diameter or bubble frequency. More recently, Nishio et al. [2] have shown that contact line density correlates well with boiling heat flux around CHF. Yet, there is no consensus which of the suggested parameters are most important in determining boiling heat transfer.

A brief review of selected experimental and theoretical studies will be given next in order to put the scope of the present work into proper perspective.

1.1. Experimental studies

Beginning with the seminal photographic study of Gaertner [3], much of our understanding about boiling processes is deduced from the *observation and interpretation of the evolution of the liquid–vapor interface*. For example, nucleation sites are detected by observing the initial growth phase of vapor embryos at the heater surface at low superheats [4, 5]. Thin heater experiments employing liquid crystal thermography [6] or sapphire glass heaters [2] provide valuable insight into the structure of liquid and vapor covered areas at the surface; however, one has to proceed with care with extrapolations to technically relevant thick heaters. *Optical*

* Corresponding author.
E-mail address: marquardt@lpt.rwth-aachen.de (W. Marquardt).

1290-0729/$ – see front matter
doi:10.1016/j.ijthermalsci.2004.04.014

Nomenclature

A	area segment of heater surface for one equivalent vapor patch
A_H	total area of heater surface
A_i	interfacial area density
c	parameter or heat capacity
C	curve or parameter
C^*	parameter
$\widehat{C}$	parameter
C_A, C_B	parameter
d	parameter
d_B	bubble diameter
d_S	equivalent dry patch size
dc_i	functional determinant of interfacial curve C_i
f	arbitrary smooth function or frequency
F	arbitrary function
g	geometry function
h	auxiliary geometry function
H	macrolayer thickness
j	index
k	index
L	equivalent dry patch distance or liquid phase
L_i	interfacial line density
$\vec{n}$	normal unit vector
N	equivalent number of dry patches
N_p	number of phase changes
$\vec{p}$	vector of equivalent key geometrical quantities
q	heat flux or parameter
Q	heat conducted from heater surface to interface
r	auxiliary geometry function
R	radius of dry patch or residual
S	surface
S_C	surface defining curve C
$\mathrm{d}s_i$	functional determinant of interfacial area S_i
t	time
T	time interval
v_C	characteristic velocity of interface
$\vec{v}$	velocity vector
V	volume or covariance matrix of parameters or vapor phase
$\vec{x}$	coordinate vector
X	phase indicator function
$\vec{y}$	vector of averaged key interfacial quantities
z	coordinate perpendicular to heater surface

Greek symbols

α	volume or time fraction
δz	appropriate distance along z
Δh_{vap}	latent heat of vaporization
$\Delta\tau$	appropriate time interval
ΔT	superheat
$\Delta\vec{T}$	superheat for different operating points along boiling curve
Δz	distance to heater surface
ρ	density
ν	normal velocity
φ	azimuthal angle
ϕ	contact angle
σ	normalized standard deviation of a parameter
Θ	parameter matrix

Subscripts

0	at heater surface, i.e., $z = 0$
1, 2, 3, 4	numbers to distinguish parameters or functions
i	interface
j	index
k	index
L	liquid phase
M	measured
S	parallel to heater surface
V	vapor phase

Superscripts

T	time average
V	volume average

probes are the only means to measure interfacial phenomena in terms of liquid–vapor fluctuations very close to the surface of both thin or thick heaters. Thus, they provide the only data base to extract useful information about the interfacial evolution in boiling processes on technically relevant heaters. Shoji measured vapor–liquid fluctuations in boiling using an impedance probe to infer vapor fraction, bubble departure frequency and macrolayer thickness from the magnitude of the signals in an attempt to verify the macrolayer evaporation correlation [7]. Precise contact frequency and vapor fraction measurements of vapor–liquid fluctuations along the entire boiling curve for various distances to the heater have been carried out by Hohl et al. [8] using a single-sensor optical probe. Buchholz et al. [9] recently carried out even more refined measurements using a four-sensor optical probe and arrays of microthermocouples embedded close to the boiling surface.

1.2. Theoretical investigations

Direct simulation of the heat, momentum and mass transfer of the boiling process at low heat fluxes (e.g., [10]) underlines that local heat and mass transfer depends largely on the evolution of the interfacial geometry. Microlayer theory predicts that much of the heat in a boiling process is transferred in the micro-region of the three-phase contact line by evaporation [11], but at high heat fluxes the complex interfacial behaviour renders direct numerical simulation difficult and predictions of the microlayer theory less accurate as bubble

number densities and departure diameters are not accessible by visual observation experimentally. The influence of the contact angle on boiling heat transfer [12] and its importance for transfer phenomena at the three-phase contact line is well known [13,14]. Dhir et al. [15] have incorporated the contact angle in their macroscopic geometry model and assumed that all the heat conducted into the liquid adjacent to the surface is used for evaporation at the interface of the vapor stems. Despite these well established theoretical approaches, the interfacial geometry and associated transfer phenomena close to the boiling surface for the entire boiling curve have not yet been identified from experimental probe data. Hence, we still lack a *verified geometry and heat transfer model* valid along the entire boiling curve, which is sufficiently simple to comply with the limited *experimental resolution*. Such a simple model is mandatory if its verification is considered an essential part of the model building activity.

1.3. Objectives and scope

Our goal is to discern the crucial parameters for the interfacial transfer phenomena in the boiling process by identifying the wetting structure, i.e., the geometry of the liquid–vapor interface close to or at the boiling surface, from experimentally accessible quantities. We believe that the interfacial geometry is a key to a better mechanistic understanding of the interfacial transfer phenomena in boiling processes and a key to the development of new heat transfer models. To achieve this goal we interpret geometry modeling and optical probe measurements [8] in the two-phase flow close to the heater surface by applying *multiphase flow averaging theory* [16–19]. The optical probe measurements which are considered in this study have been conducted with a single sensor probe with a tip diameter of 10 μm in pool boiling of FC-72 on a test heater which consisted of an electrically heated copper block with 35 mm diameter and 10.5 mm thickness [8]. Multiphase flow averaging theory provides instruments to adapt the level of detail suitable for modeling and experimentation. *By assuming an ergodic and stationary boiling process* physically meaningful quantities of the interfacial structure are obtained by applying time-averaging to sensor probe data [8].

Such quantities can be obtained from purely geometrical considerations by means of area- or volume-averaging. In particular, we consider vapor fraction, interfacial line and area densities and their respective fluxes as important quantities. Based on mathematically rigorous definitions of these quantities, a regression problem is formulated and solved in order to correlate unmeasurable relevant geometrical parameters such as the average size of vapor spots and nucleation site density as a function of superheat using measured vapor fractions and interface contact frequency along the entire boiling curve. For this purpose, a simple geometry model of the interfacial structure is employed to capture the underlying geometries of many modeling approaches [15,20] in a unifying manner. This study reveals that many relevant parameters suggested for correlating boiling heat flux are linked to each other by a mathematical model of the interfacial geometry. In the most simple case, only a single unknown is left which is closely related to a characteristic interfacial velocity. In this study, this unknown is assumed constant along the entire boiling curve lacking a measurement to deduce this quantity from.

In the second part, a new correlation is suggested, which describes the boiling heat flux as a function of interfacial area density or its flux and superheat employing only a single fitting parameter in its most simple form. Interfacial area flux is directly related to the contact frequency of liquid–vapor fluctuations measured by optical probes and can be interpreted as a measure for the evaporation rate. It is shown that the new correlative quantity even seems to account for the dependence of boiling heat transfer on the equilibrium contact angle. The new correlation is compared to and discriminated against existing correlations to assess their relative merit.

2. Model geometries for boiling processes

Over the past decades different geometry models for the near-wall boiling process have been suggested. The two most important geometries which have been assumed to idealize the liquid-rich "macrolayer" are "vapor stems" as in the model of Dhir et al. [15] or "bubbles" as suggested and discussed by Sadasivan et al. [20]. Both geometries have been used in subsequent approaches, e.g., [21].

Dhir and Liaw [15] assumed that stationary vapor stems grow in a regular, square grid at the boiling surface spaced a distance L apart as shown in Fig. 1 (left). The vapor stems are characterized by their diameter d_S. The stems can merge when $d_S/L > 1$.

The "bubble geometry" consists of spheres with diameter d_B residing on the boiling surface spaced a distance L apart as shown in Fig. 1 (right). An additional parameter accounts for the distance H of the sphere's center to the boiling surface. This distance also defines the macrolayer thickness, i.e., the point where coalescence of the bubbles is assumed to occur. This geometry model has also been used much earlier to correlate CHF [22].

Both models assume a particular geometry with particles of equal shape and relative position. Three parameters $\{d_S, L, \phi\}$ or $\{d_B, L, H\}$ are required to completely describe the situation. Obviously, the true wetting structure is much more complicated and changes dramatically along the boiling curve. First, the true interface of a single vapor chunk will be much more irregular in the upper nucleate and transition boiling regions. Second, the structures will not be of a single type with a regular spatial arrangement. Therefore, the simple geometry models have to be understood to equivalently represent the much more complicated wetting behaviour in some averaged sense. Consequently, these parameters should be understood as *expected values of as yet*

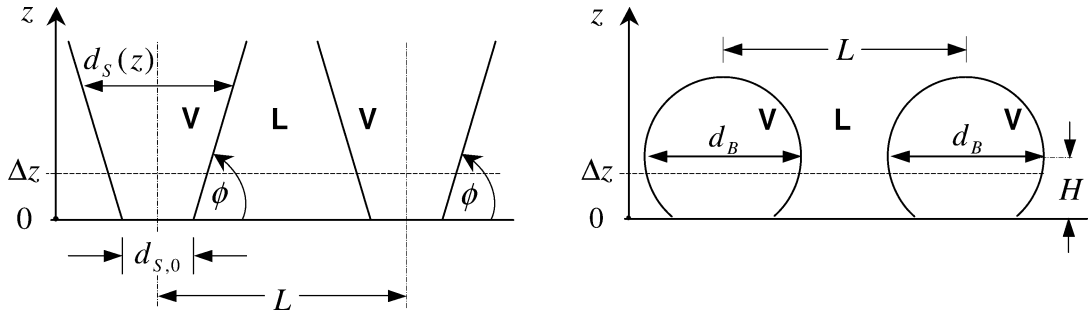

Fig. 1. Geometry model of Dhir et al. [15] for separated stems (left), bubble geometry model by Sadasivan et al. [20] (right).

unknown statistical distributions. Their meaning should become even more obvious through the detailed discussion in Sections 3–5. These models can be considered as minimal parameterizations for constituting a boiling process geometry. If these models are applied along the boiling curve, the parameters become functions of superheat. The major difference between both models is the treatment of interfacial curvature.

Until now, we are faced with the following difficulties and still unresolved problems:

(1) Parameters such as the macrolayer thickness have mainly been used for modeling critical heat flux, but the development of a mechanistic model or correlation of boiling heat transfer should involve parameters that do not limit their applicability to a certain boiling regime. This has already been pointed out before [23].
(2) Modeling boiling heat transfer using different geometry models makes comparison of results and discussion of mechanistic effects very hard or even impossible.
(3) The parameters used in the models cannot be measured directly such as a typical diameter of a vapor phase structure or the macrolayer thickness.
(4) Due to the fact, that many parameters are not measurable directly, they have sometimes been inferred by a rough interpretation of sensor signals such as the macrolayer thickness deduced from probe data [7]. Therefore, an important issue is to relate experimentally available probe data to the models in a mathematically rigorous way.
(5) The dependence of the interfacial geometries and therefore the parameters of the underlying wetting structure with superheat is still unknown. The necessity for the development of a theoretical or empirical model for the surface wettability as a function of surface condition, temperature and transport rates has very recently been emphasized [24].
(6) Additional difficulties arise if data are not readily available in the same experiment. In theoretical studies, this data must then be taken from different sources typically encoded by vague correlations. As a consequence, a lot of these studies suffer from a higher potential of inconsistencies due to the well-known difficulties in precise control of experimental parameters. Even worse, sometimes physically related quantities are mixed without worrying about their relationship. This makes results of simulation studies less reliable and less amenable for proper interpretation of mechanistic effects.

As a consequence, many assumptions underlying some of the present models have not yet been verified.

In our approach, we try to avoid these shortcomings as much as possible. As already pointed out, multiphase flow averaging theory defines averaged geometrical quantities. This theory applies to arbitrary geometries including those shown in Fig. 1 and equally well to the interpretation of experimental data. The average quantities are introduced in the next section. Although it would be a desirable goal to discriminate between alternative model geometries, it will become clear that such a discrimination is not advisable based on single sensor probe experimental data [8] which we are going to employ. Instead, we here focus on identifying the interfacial geometry at a distance Δz above the heater surface (Fig. 1) as a first step. In this case, both models become indistinguishable and show the same geometrical parameters. Thereby, we avoid parameters that depend on the geometrical perception in three dimensions. This way we are able to explore whether the identification of the wetting structure by means of highly simplified models is successful to discern key parameters of the boiling process. Therefore, instead of mere simulation the formulation and solution of an inverse problem is suggested. Some questions of identifiability are addressed. Finally, these results are utilized to compare correlating quantities for the entire boiling curve. The correlating quantities and the boiling curve are obtained from the same experimental setup [8].

3. Averaged geometrical modeling

One way to study the behaviour of boiling processes is to follow the details of the interfacial evolution, e.g., by direct numerical simulation. Except for low heat fluxes this is not practical due to the complex nature of the process. Furthermore, due to the natural variability in physical systems initial and boundary conditions are often not known and cannot be controlled precisely. Consequently, the accuracy of the computed fields of pressure, velocity etc. is limited by the ac-

curacy of the boundary and initial conditions used for their computation. Second, it would be difficult to verify the excessive amount of field information from detailed numerical computations experimentally.

Averaging theory allows the interpretation of phenomena in terms of repeated experiments and expected values of their outcome. It provides mathematically rigorous definitions and sets of equations in an averaged sense to describe the macroscopic motion of a flow. The microscopic details reflecting the essential physics cannot be recovered from the averaged quantities. However, the gross details of the relevant phenomena are not lost, as they will be contained in the statistics of the averaged parameters and constitutive equations of the macroscopic model. For more details we refer to Ishii [18] or Drew and Passman [17]. Multiphase flow averaging theory provides mathematically defined averaged geometrical quantities in terms of volume-, area- and time-averaging. Averaging makes it possible to suitably adapt the level of detail in the models to experimental resolution and to compare differently averaged quantities if an ergodic process is assumed.

Ergodicity is important for the development of a model for the boiling process. The ergodicity assumption allows volume- or area-averaged quantities obtained from a process model which is based on *stationary, average geometry* considerations to be related to averaged quantities obtained from *local measurements based on time-sampling*.

In an ergodic process, the time-averaged quantity

$$\bar{f}^T(\vec{x}) = \lim_{T\to\infty} \frac{1}{T} \int_T f(\vec{x}, t)\,\mathrm{d}T \tag{1}$$

equals the instantaneous, volume averaged quantity

$$\bar{f}^V(t) = \lim_{V\to\infty} \frac{1}{V} \int_V f(\vec{x}, t)\,\mathrm{d}V \tag{2}$$

Hence, $\bar{f}^T(\vec{x}) = \bar{f}^V(t)$ for ergodic processes. Applying ergodicity a second time yields the identity

$$\overline{\bar{f}^T}^V = \overline{\bar{f}^V}^T \tag{3}$$

As a consequence ergodicity is of fundamental importance as it links a geometrical view of the two-phase flow to experimental probing techniques. Consider, for example, an irregular distribution of an ensemble of vapor chunks across the boiling surface. The distribution instantaneously present on the surface may change with time. Observing a sufficient number of vapor chunks randomly picked from the ensemble at a particular point at or close to the surface over a long time period will not differ from observing a representative large number of vapor chunks in the same ensemble distributed across the surface. Therefore, it will not matter if time- or space-averaging is pursued and which is going to be performed first. Moreover, the averages obtained by time- or space-averaging will be the same, even if a complex vapor chunk ensemble is replaced by a much simpler one, if it is equivalent with respect to the expected macroscopic quantities. Such simple geometries consisting of equal vapor chunks are considered here. Examples have been presented in Fig. 1.

Subsequently, some definitions of averaged geometrical quantities using volume-, area- and time-averaging are recalled as they are necessary for our purposes.

3.1. Volume- and area-averaged geometrical quantities

Interfacial evolution is characterized by the normal interfacial velocity $v(\vec{x}, t)$ and the normal unit vector $\vec{n}(\vec{x}, t)$ at the interface. The evolution of the interface obeys a kinematic or topological equation.

Instead of treating a general interfacial geometry we consider the specific geometry shown in Fig. 2 which might be considered as an idealized vapor chunk. This interfacial geometry neglects curvature along the z-direction, but considers the contact angle ϕ of the wetting liquid. It complies with the geometrical model of Dhir et al. [15] (cf. Fig. 1 (left)). The definitions of averaged quantities, orginally developed as part of the averaging theory of Delhaye [16] and others, are applied directly to the geometry in Fig. 2 in order to point out the different properties of the averaged quantities with respect to boiling process modeling. The definitions are employed later to correctly relate model quantities to available experimental probe data, to distinguish them for the identification of equivalent geometrical quantities as well as to develop and discriminate heat transfer correlations.

In this geometry, S_i denotes the interfacial surface, C_i denotes a curve defined by an arbitrary cross-sectional plane S_C located at some distance z parallel to the surface S_0. $\vec{n}_i$ is the outward normal unit vector to the interface S_i, $\vec{n}_{iS}$ is the outward normal unit vector to the interface S_i tangential to the cutting plane S_c. A local cylindrical (R, φ, z)-coordinate system is introduced with the z-direction chosen along the stem's axis, i.e., normal to S_0. The radius of the interface at the surface S_0, i.e., $z = 0$, is denoted by R_0. The radius of the interface depends on z and is therefore denoted by $R(z)$. It is determined by the contact angle ϕ at the surface S_0.

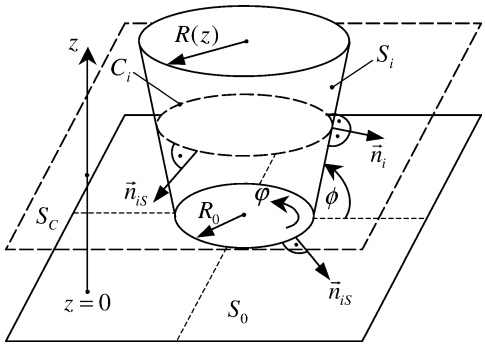

Fig. 2. Three-dimensional "stem-like" interfacial geometry with a planar interface.

We define the area-averaged line density of the stem periphery as

$$L_i = \frac{1}{A} \int\limits_{C_i(\vec{x},t)} \vec{n}_{iS} \cdot \vec{n}_{iS}\, \mathrm{d}c_i(\vec{x},t) \tag{4}$$

where $\vec{x}, \vec{n}_{iS} \in \mathbb{R}^2$. A is an area segment of the boiling surface over which the average is taken for a single vapor chunk and $\mathrm{d}c_i(\vec{x},t)$ is the functional determinant of curve C_i [25]. For the cylindrical coordinate system chosen and the geometry assumed in Fig. 2, we have

$$\mathrm{d}c_i(\vec{x},t) = \left| \frac{\partial \vec{x}}{\partial \varphi} \right| \tag{5}$$

with $\vec{x}$ describing the curve C_i in cylindrical coordinates, i.e.,

$$\vec{x} = \begin{pmatrix} (z\tan^{-1}\phi + R_0)\cos\varphi \\ (z\tan^{-1}\phi + R_0)\sin\varphi \end{pmatrix} \tag{6}$$

Finally, we can write for the line density at z,

$$\begin{aligned} L_i(z,t) &= \frac{1}{A} \int\limits_{\varphi=0}^{\varphi=2\pi} \left(z\tan^{-1}\phi + R_0\right) \mathrm{d}\varphi \\ &= \frac{2\pi}{A}\left(z\tan^{-1}\phi + R_0\right) \end{aligned} \tag{7}$$

Accordingly, an interfacial area density is defined by

$$A_i = \frac{1}{V} \int\limits_{S_i(\vec{x},t)} \vec{n}_i \cdot \vec{n}_i\, \mathrm{d}s_i(\vec{x},t) \tag{8}$$

with $\vec{x}, \vec{n}_i \in \mathbb{R}^3$. $\mathrm{d}s_i$ is the surface element defined as

$$\mathrm{d}s_i(\vec{x},t) = \left| \frac{\partial \vec{x}}{\partial \varphi} \times \frac{\partial \vec{x}}{\partial z} \right| \tag{9}$$

with $\vec{x}$ describing the interfacial geometry in cylindrical coordinates, i.e.,

$$\vec{x} = \begin{pmatrix} (z\tan^{-1}\phi + R_0)\cos\varphi \\ (z\tan^{-1}\phi + R_0)\sin\varphi \\ z \end{pmatrix} \tag{10}$$

for the geometry assumed in Fig. 2. Using Eqs. (9), (10) we obtain

$$\mathrm{d}s_i(\vec{x},t) = \sqrt{1+\tan^{-2}\phi}\left(z\tan^{-1}\phi + R_0\right) \tag{11}$$

The interfacial area density close to the boiling surface at z can be obtained from

$$\begin{aligned} &A_i(z,t,\delta z) \\ &\quad = \frac{1}{2A\delta z} \int\limits_{z-\delta z}^{z+\delta z} \int\limits_{\varphi=0}^{\varphi=2\pi} \frac{z\tan^{-1}\phi + R_0}{(\sqrt{1+\tan^{-2}\phi})^{-1}}\, \mathrm{d}z\, \mathrm{d}\varphi \end{aligned} \tag{12}$$

where we have taken the average over a volume element $V = 2\delta z A$. The square root $\sqrt{1+\tan^{-2}\phi}$ can be simplified to $\sin^{-1}\phi$ and taken outside the integral as it does not depend on z nor on φ according to Fig. 2. In order to apply the averaging over an infinitesimally small volume, we take the limit $\delta z \to 0$ of Eq. (12). Hence, we obtain

$$A_i(z,t) = \frac{2\pi}{A\sin\phi}\left(z\tan^{-1}\phi + R_0\right) \tag{13}$$

The area-averaged vapor fraction is given by

$$\begin{aligned} \alpha_V(z,t) &= \frac{1}{A} \int\limits_{A_V} \mathrm{d}A_V \\ &= \int\limits_{\varphi=0}^{2\pi} \int\limits_{r=0}^{z\tan^{-1}\phi + R_0} r\, \mathrm{d}r\, \mathrm{d}\varphi \end{aligned} \tag{14}$$

yielding

$$\alpha_V(z,t) = \frac{\pi}{A}\left(z\tan^{-1}\phi + R_0\right)^2 \tag{15}$$

The area-averaged vapor fraction may also be deduced from a volume-averaged fraction in the limit of vanishing thickness of the control volume. This is in contrast to line and area density, where the area density does not converge to the line density in the limit of an infinitesimally small control volume.

3.2. Contact angle

Using the above definitions of line and area density for the assumed geometry, it can easily be shown that the line and area density at the boiling surface are simply related by the contact angle ϕ.

Comparing Eqs. (7) and (13), we find that the ratio of interfacial area density A_i and line density L_i at a certain position z of the cutting plane depends on the contact angle ϕ according to

$$\frac{L_i(z,t)}{A_i(z,t)} = \sin\phi \tag{16}$$

It can be shown that at the boiling surface, i.e., at $z = 0$, the same result as in Eq. (16) would have been obtained for geometries with an *arbitrary curvature*. The importance of the contact angle for condensation and evaporation is well known. We will discuss the implications regarding the correlation of boiling heat flux later.

4. Interpretation of sensor probe experiments

Sensor probing is a *local*, *pointwise* measuring technique. Sensors of a probe ideally measure the phase indicator function $X(\vec{x},t)$ which signals the presence of the vapor (V) or the liquid phase (L) at the probe tip location $\vec{x}$ at the time instant t. Mathematically, this can be expressed as

$$X(\vec{x},t) = \begin{cases} 0 & (\vec{x},t) \in L \\ 1 & (\vec{x},t) \in V \end{cases} \tag{17}$$

The phase indicator function carries *two independent* pieces of information over time: the time instance of phase change to a particular phase and the time duration of its presence.

4.1. Time-averaged geometrical quantities

The vapor fraction α_V is determined in terms of time averaging as

$$\alpha_V = \frac{1}{\Delta\tau}\int_t^{t+\Delta\tau} X\,\mathrm{d}t \tag{18}$$

in case the ergodicity assumption holds. Ishii [18] suggests to determine the interfacial area density A_i from

$$A_i = \frac{1}{\Delta\tau}\sum_j\left(\frac{1}{|\vec{v}_i\cdot\vec{n}_i|}\right)_j \tag{19}$$

where the summation is taken over all j instances of interfacial contacts at point $\vec{x}$ during the time interval $\Delta\tau$. $\vec{v}_i\cdot\vec{n}_i$ is the scalar product of interfacial velocity $\vec{v}_i$ and the normal unit vector $\vec{n}_i$ of the interface at point $\vec{x}$. This product will also be denoted by $v(\vec{x},t)$, the normal interfacial velocity. This equation is based on the theory of two-phase flow where the interface is assumed to have negligible thickness. The interfacial area density A_i can be inferred from four-sensor probe measurements [26].

According to Delhaye [16], the time rate of change of the vapor fraction can be expressed as

$$\frac{\partial\alpha_V}{\partial t} = \frac{1}{\Delta\tau}\sum_j\left(\frac{\vec{v}_i\cdot\vec{n}_i}{|\vec{v}_i\cdot\vec{n}_i|}\right)_j \tag{20}$$

Drew [27] has shown the equivalence

$$\frac{\partial\alpha_V}{\partial t} = A_i v \tag{21}$$

with the interfacial area flux $A_i v$. In the averaging theory of two-phase flows, all transfer terms between the phases are proportional to the interfacial area flux $A_i v$ relative to the interfacial area density weighted phase velocity at the interface. In the case of two-phase flows with evaporation such as boiling processes, the mass transfer between the phases can be obtained by multiplying the difference between the interfacial area density weighted phase and interface velocity with a phase density. Hence, there is a very close connection of an evaporation rate to the interfacial area flux. The interfacial area flux or time rate of change of the vapor fraction, which can be determined simply by the sum of the positive and negative signs of the projection of the interfacial velocity $\vec{v}_i$ normal to the interface, may therefore be interpreted as measure of evaporation in a boiling process.

4.2. Approximation of average geometrical quantities for single sensor probe experiments

A single optical probe allows measurements of a single characteristic function X in contrast to four-sensor probe measurements. No interfacial velocity information can be deduced from single sensor probes. In order to interpret the single optical sensor probe data of Hohl et al. [8], who measured contact frequencies f and vapor fractions α_V, we introduce a pragmatic approximation for the interfacial area density A_i, Eq. (19):

$$A_i = C_1^* f = C_1^*\frac{N_p}{\Delta\tau} \tag{22}$$

The contact frequency f replaces the summation over all instances j in Eq. (19) under the assumption that an averaged normal interfacial velocity is of sufficient accuracy. The contact frequency is the ratio of the number of phase changes N_p and measurement time $\Delta\tau$. C_1^* is an unknown parameter.

The line density L_i can be approximated in a similar way. Obviously,

$$L_i = C_2^*\frac{N_p}{\Delta\tau} \tag{23}$$

The parameter C_2^* may be interpreted as the reciprocal of an unknown characteristic average interfacial velocity. This velocity has to be chosen appropriately since it cannot be inferred from single sensor probe measurements. This characteristic velocity relates space and time scales of the process and is suspected to be closely related to the interfacial normal velocity of the evaporation process. We will denote this characteristic velocity with $\overline{v_C}$ and write

$$C_2^* = \frac{1}{\overline{v_C}} \tag{24}$$

It might be a function of the distance to the boiling surface and of the superheat ΔT in a boiling process. Using Eq. (16) the relation between C_1^* and C_2^* is given as

$$C_2^* = C_1^*\sin\phi \tag{25}$$

In addition, the contact frequency f might be used to approximate the interfacial area flux according to Eqs. (20) and (21) as

$$A_i v = \frac{1}{\Delta\tau}\sum_j\left(\frac{\vec{v}_i\cdot\vec{n}_i}{|\vec{v}_i\cdot\vec{n}_i|}\right)_j = C_3^*\frac{N_p}{\Delta\tau} = C_3^* f \tag{26}$$

This equation suggests that the *contact frequency measured close to the heated surface using a single sensor probe may be related to the rate of evaporation* by an unknown parameter C_3^*. This parameter accounts for the fact that a single optical probe cannot measure the sign of the normal interfacial velocity. This parameter is dimensionless and might again depend on the distance to the boiling surface and superheat. In some situations, e.g., very close to the wall, C_3^* might be trivial to determine, but generally its determination is complicated or even impossible even if an array of sensors is employed to determine the sign of normal velocity at the interface v. For example, if the normal velocity is caused by two physical phenomena, e.g., by evaporation and by an upward oriented motion of the particle, the second piece of information, another positive normal interfacial velocity, required to conclude that there is evaporation, may not be detected at the same probe tip, unless the upward oriented motion becomes again faster than the evaporation. But then, the normal interfacial velocity is determined by the upwards

motion with a negative normal velocity. Therefore, specially designed probe assemblies and signal processing schemes will be required for proper determination of $A_i v$.

According to the approximations in this section, we find that one cannot distinguish between interfacial area flux $A_i v$, interfacial area density A_i or line density L_i from single sensor probe measurements which only provide the phase indicator function (17). However, we may derive approximations for these quantities from contact frequency measurements derived from (17) subject to the unknown quantities C_k^* which at least depend on the distance z of the sensor tip from boiling surface and the superheat ΔT. These approximations will be used subsequently for the identification of the interfacial geometry.

5. Multi-vapor spot geometry model

As already pointed out at the end of Section 2, a simple geometry model unifying both the stem and the bubble model is chosen in this study. This model describes the geometry as shown in Fig. 3 in a cutting plane at a position z parallel to the boiling surface (see Fig. 2). The geometry is parameterized by a characteristic size, i.e., the diameter d_S of "vapor spots" and their distance L, and assumes N vapor spots close to a heater's whole surface area A_H which is assumed to be a square. Coalescence occurs at $d_S \geqslant L$. If coalescence is ruled out, $d_S < L$. The interfacial area density and vapor fraction for the two cases are given by

$$g_1\colon\ A_i = \frac{\pi d_S}{L^2}\left(1 - h_1\left(\frac{d_S}{L}\right)\right)\sin^{-1}\phi$$
$$\text{with}\quad \begin{cases} h_1 = 0 & d_S \leqslant L \\ h_1 = \frac{4}{\pi} r\left(\frac{d_S}{L}\right) & d_S > L \end{cases} \tag{27}$$

$$g_2\colon\ \alpha_V = \frac{\pi d_S^2}{4L^2}\left(1 - h_2\left(\frac{d_S}{L}\right)\right)$$
$$\text{with}\quad \begin{cases} h_2 = 0 & d_S \leqslant L \\ h_2 = \frac{4}{\pi} r\left(\frac{d_S}{L}\right) - \frac{2}{\pi}\sin\left(2r\left(\frac{d_S}{L}\right)\right) & d_S > L \end{cases} \tag{28}$$

and with the abbreviation function

$$r\left(\frac{d_S}{L}\right) = \arcsin\sqrt{1 - \left(\frac{L}{d_S}\right)^2} \tag{29}$$

For $0 \leqslant d_S/L \leqslant 1$ the functions g_1 and g_2 can be obtained from Eqs. (13) and (15) using the substitutions $d_S = 2R(z) = 2(z\tan^{-1}\phi + R_0)$ and $A_H = NA = NL^2$. Using Eq. (16) line densities can be obtained from Eq. (27). The relation between nucleation site density N/A_H, line and area density and vapor fraction is pure geometry. Nucleation site density can be expressed in terms of the other geometrical variables as

$$\frac{N}{A_H} = \frac{1}{L^2} = \frac{A_i^2 \sin^2\phi}{4\pi\alpha_V} h_3\left(\frac{d_S}{L}\right)$$
$$\text{with}\quad \begin{cases} h_3 = 1 & d_S \leqslant L \\ h_3 = \frac{1 - \frac{4}{\pi} r\left(\frac{d_S}{L}\right) + \frac{2}{\pi}\sin\left(2r\left(\frac{d_S}{L}\right)\right)}{\left[1 - \frac{4}{\pi} r\left(\frac{d_S}{L}\right)\right]^2} & d_S > L \end{cases} \tag{30}$$

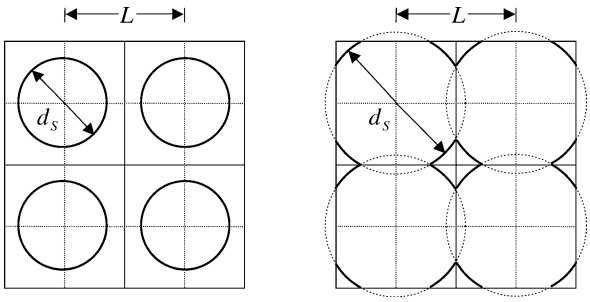

Fig. 3. Interfacial geometry model for the cutting plane at Δz (see Fig. 2): without coalescence (left), with coalescence (right).

A nucleation site can be understood as the center of the vapor spots of the employed geometry model.

In this framework, the nucleation site density, the diameter and spacing should be understood as equivalent quantities that are introduced to idealize and simplify the much more complex actual interfacial structure of the process. In terms of averaging, the equivalent quantities are understood to lead to the same vapor fraction and interfacial area densities as the wide distributions of the many more or less irregular interfacial events which occur in the actual situation. Hence, d_S and L may not be interpreted as a single event of the process since the spatial scales of a single event may vary in orders of magnitude and behave much more complicated.

6. Identification of interfacial geometry close to the surface

The interfacial geometry model (see Fig. 3) is now used to identify the equivalent vapor spot diameter d_S and spacing L close to the heater surface using experimental single probe data of Hohl et al. [8]. The data consists of time averaged vapor fractions $\alpha_{V,M}$ and contact frequencies f_M measured at eight different superheats $\Delta\vec{T} = (20; 25; 30; 35; 40; 45; 50; 80)^{\mathrm{T}}$ K and six different distances to the boiling surface, i.e., $\vec{z} = (0.01; 0.03; 0.05; 0.1; 0.5; 1.0)^{\mathrm{T}}$ mm at three different locations across the heater's surface. Among the three different locations only slight variations in the time averaged vapor fraction and contact frequency was found. Whereas the two innermost positions (middle, and 8 mm from the middle of the heater), especially at distances very close to the boiling surface, showed only very small differences in the variations of the time averaged quantities with superheat, the time averaged quantities at the outermost position at 3 mm from the heater's boundary, showed a somewhat more pronounced difference of the time averaged vapor fraction and contact frequency compared to the two other. However, even among the outer- and innermost lateral positions the variations were always much less pronounced than the variation of the time averaged quantities at all positions because of superheat. Therefore, we conclude that the boiling process was quite homogeneous across the whole boiling surface, where only

the outermost position was maybe influenced by some sort of end-effect.

Depending on the geometrical parameter vector $\vec{p} = (d_S, L)^{\mathrm{T}}$, the geometrical model $\vec{g}$ given in Eqs. (27)–(29) predicts area densities A_i and vapor fractions α_V and is written as

$$\vec{y} = \begin{pmatrix} A_i(\vec{p}) \\ \alpha_V(\vec{p}) \end{pmatrix} = \begin{pmatrix} g_1(\vec{p}) \\ g_2(\vec{p}) \end{pmatrix} \tag{31}$$

Note, that the contact angle ϕ is not included in the parameter vector $\vec{p}$ since ϕ is not identifiable from single sensor probe data which we are going to employ. Instead ϕ is included in the unknown characteristic velocity as dicussed below. Both d_S and L are unknown functions of the superheat ΔT which could in principal behave arbitrarily. Hence, we should use fairly general functions for describing the dependency, e.g., by piecewise linear functions or splines. However, we simply choose a linear dependency here and introduce

$$\vec{p}(\Delta T) = \begin{pmatrix} d_S(\Delta T) \\ L(\Delta T) \end{pmatrix} = \begin{pmatrix} c_1 & d_1 \\ c_2 & d_2 \end{pmatrix} \begin{pmatrix} \Delta T \\ 1 \end{pmatrix} \tag{32}$$

in order not to overparameterize the inverse problem in face of the relatively scarce measurements. The results presented later reveal that this linear dependency is sufficient to capture the data accurately. In general it might happen that d_S and L behave much more complicated such that a finer parameterization must be chosen to capture the essential behaviour. However, the resolution of the parameterization must be adapted suitably to the number of experimentally available data points. In any case, the constraint

$$0 \leqslant d_S(\Delta T)/L(\Delta T) \leqslant \sqrt{2} \tag{33}$$

must hold for all superheats for a valid geometry model, because no vapor spots exist for $d_S/L = 0$ and the vapor spots are fully coalesced for $d_S/L = \sqrt{2}$.

For the identification of the parameters $\Theta = (c_1, d_1; c_2, d_2)$ we use the time-averaged vapor fraction $\alpha_{V,M}$ and the contact frequency f_M measured by Hohl et al. [8]. In order to minimize the variance of the data, we arithmetically average the data measured at a distance of $z = 0.01$ mm and $z = 0.03$ mm to the boiling surface both in the middle of heater as well as at 8 mm distance from the middle of the heater. According to Eqs. (22)–(25) which lead to

$$A_i = C_1^* f = \frac{C_2^*}{\sin\phi} f = \frac{1}{\bar{v}_C \sin\phi} f \tag{34}$$

we can obtain an averaged area density $A_{i,M}$ from the measured contact frequency f_M if the characteristic interfacial velocity $\bar{v}_C$ and the contact angle ϕ would be known. Unfortunately, there is no means to identify these quantities from the available experimental probe data. Multi-tip probes would be required for this purpose. Both quantities are therefore combined into $v_C = \bar{v}_C \sin^{-1}\phi$. Recent experimental results by Buchholz et al. [9] indicate velocity values between 400 mm·s^{-1} and 1000 mm·s^{-1} at a distance between 4.5 mm and 20 mm from the boiling surface. If this data is extrapolated linearly to the boiling surface, a velocity of approx. 200 mm·s^{-1} is obtained. This velocity might serve as a first clue for v_C, but needs further verification. Both measured area density and vapor fraction are included in the measurement vector

$$\vec{y}_M(\Delta T_k) = \begin{pmatrix} A_{i,M}(\Delta T_k) \\ \alpha_{V,M}(\Delta T_k) \end{pmatrix} = \begin{pmatrix} f_M(\Delta T_k)/v_C \\ \alpha_{V,M}(\Delta T_k) \end{pmatrix} \tag{35}$$

The problem of the identification of the unknown parameter matrix Θ and hence the functional dependency of $d_S(\Delta T)$ and $L(\Delta T)$ is formulated as the constrained regression problem

$$\min_{\Theta} \sum_{k=1}^{7} \left(\vec{y}\left(\vec{g}\left(\vec{p}(\Theta, \Delta T_k)\right)\right) - \vec{y}_M(\Delta T_k)\right)^2 \tag{36}$$

$$\text{s.t. Eqs. (31)–(35)} \tag{37}$$

whose solution minimizes the sum of quadratic differences between the predicted values $\vec{y}$ by the model and the measured values $\vec{y}_M$ at $k = 1, \ldots, 7$ different superheats ΔT_k. The parameter estimation problem is solved using a sequential quadratic programming method [28]. Note, that the quantities v_C and $\sin\phi$ in Eq. (25) pose the only unknown inputs in the formulation which cannot be estimated by the solution of the estimation problem. However, from an analysis of Eqs. (27) and (28) we find that the ratio $d_S(\Delta T)/L(\Delta T)$ is independent of v_C. Hence, $d_S(\Delta T)/L(\Delta T)$ is uniquely defined from the available single sensor probe data whereas the estimated d_S, L and hence N/A_H will dependent on the characteristic velocity chosen. For the extrapolated characteristic velocity $v_C = 200$ mm·s^{-1} an optimal solution is found for $\Theta = (0.068\,\text{mm·K}^{-1}, -1.352\,\text{mm};\ -0.022\,\text{mm·K}^{-1}; 2.51\,\text{mm})$. Equally good solutions are found for other characteristic velocities. Comparison between experimental data and model prediction is shown in Figs. 4 and 5.

The geometry model predicts the measured data quite well. The data points seem to be randomly distributed around the model predictions, however, for the few data points at hand the confidence in the predictions is rather poor. Therefore, it would be highly desirable to have much more data points in order to statistically verify the model, e.g., to determine the performance of the model around the maximum in interfacial area density.

From the geometric ratio $d_S(\Delta T)/L(\Delta T)$ we find that the boiling surface accretes increasingly as can be seen in Fig. 6. As already pointed out, this ratio is independent of the characteristic velocity chosen and is uniquely defined from the single optical probe data.

Figs. 7 and 8 reveal that the estimated average stem diameter d_S grows whereas the spacing L between the stems decreases with increasing superheat ΔT. As expected, stem diameter and spacing depend on the chosen velocity v_C. As shown in the Figs. 7 and 8 d_S and L are proportional to v_C.

Although the results are obtained using a constant characteristic velocity, the true interfacial velocity may depend

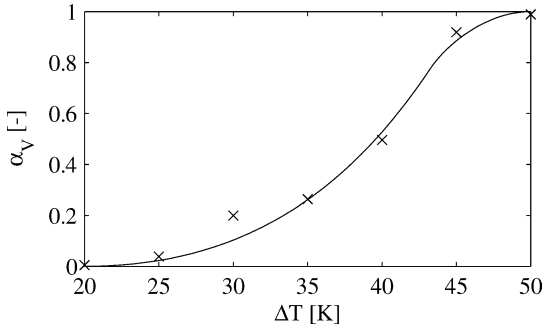

Fig. 4. Comparison between measured (symbol ×) [8] and predicted (solid line) vapor fractions for $v_C = 200$ mm·s^{-1} during boiling of FC-72.

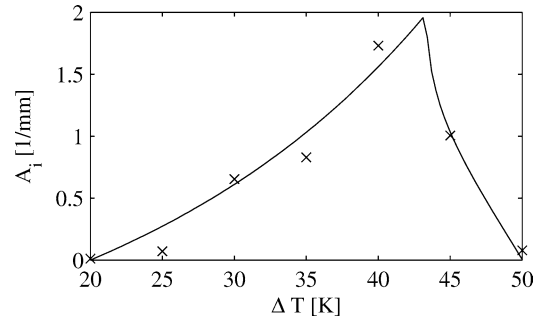

Fig. 5. Comparison between measured (symbol ×) [8] and predicted (solid line) interfacial area densities for $v_C = 200$ mm·s^{-1} during boiling of FC-72.

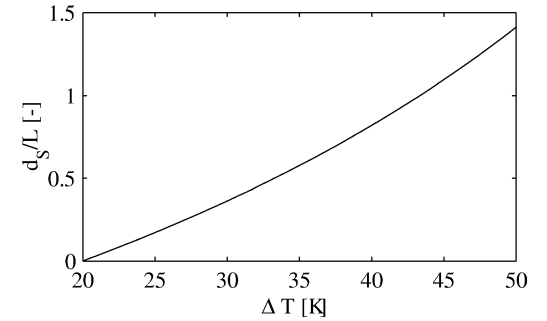

Fig. 6. Ratio of estimated stem diameter and spacing independent of v_C during boiling of FC-72.

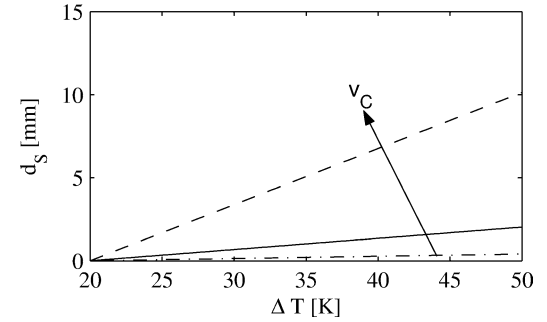

Fig. 7. Estimated stem diameter during boiling of FC-72 for $v_C = \{40, 200, 1000\}$ mm·s^{-1}.

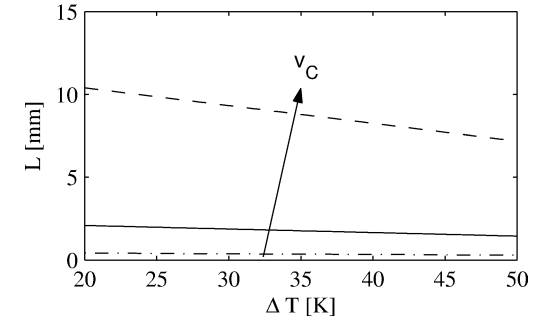

Fig. 8. Estimated stem spacing during boiling of FC-72 for $v_C = \{40, 200, 1000\}$ mm·s^{-1}.

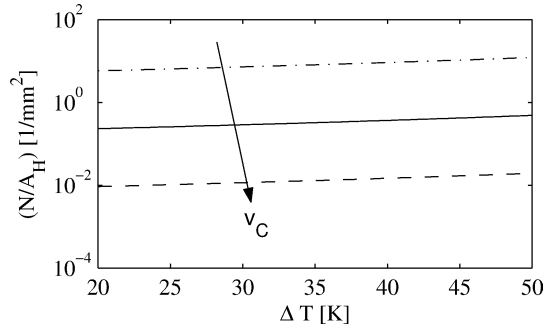

Fig. 9. Estimated nucleation site density during boiling of FC-72 for $v_C = \{40, 200, 1000\}$ mm·s^{-1}.

on the superheat. In order to validate these results and to identify $v_C(\Delta T)$ new measurements using multiple sensor probes which allow to measure interfacial velocities as a function of ΔT must be conducted.

From the identified parameters an estimate of nucleation site density can be obtained even in boiling regimes where their determination by visual observation is impossible. The estimate is shown in Fig. 9 for different characteristic interfacial velocities.

To our knowledge, no investigations have been carried out to count nucleating site density for FC-72 on a grounded copper heater at superheats above $\Delta T = 20$ K. Luke et al. [5] found active nucleation site densities in boiling propane on a fine sandblasted copper tube in the order of 2.8–10.25 mm^{-2} at heat fluxes up to 2 W·cm^{-2} and intermediate pressures. Barthau [29] measured nucleation site density on a sandblasted, gold-plated copper tube in boiling R134a between 10^{-1} and 10^{1} mm^{-2} at heat fluxes up to 2 W·cm^{-2}. The results on the estimated equivalent nucleation site densities presented here in this framework are in reasonable ranges compared to experimental investigations. However, they are very sensitive to the interfacial velocity.

7. Boiling heat transfer correlations

The results of the previous sections show that vapor fraction α_V, line density L_i, area density A_i, nucleation site density N/A_H as well as the vapor spot size d_S are related by a model of the interfacial geometry of the boiling process.

The most prominent suggested correlations use nucleation site density, vapor fraction, or line densities (e.g., Berenson [30], Nishio et al. [2]). Therefore, these correlations should no longer be regarded as independent. In fact, they are related by the interfacial geometry of the process.

Most of the empirical approaches for correlating boiling heat flux have only inferred the correlative quantities for particular parts of the boiling curve where they have been directly accessible by measurements. Therefore, existing correlations are often valid only for one of the boiling regimes and relevant physical parameters have not yet been identified which allow a simple *unifying description of the entire boiling curve*. Therefore, our next goal is to discriminate correlations in order to identify the most relevant physical parameters. We suggest a new correlation which covers all boiling regimes and qualitatively includes the relevant physical effects, i.e., evaporation and micro-convection associated with the interfacial and contact line movement, but requires further quantitative verification. This correlation is based on interfacial area density A_i or its flux $A_i v$.

7.1. A new boiling heat transfer correlation

The new correlation suggested which is based on interfacial area density or its flux can be interpreted as a measure of transport phenomena associated with the presence of an interface as well as with interfacial movement, e.g., during evaporation. Indeed, the interfacial area flux is a measure for the rate of evaporation (cf. Eqs. (20), (21)) and is related to the measured contact frequency despite an unknown parameter according to Eq. (26). Compared to line densities L_i, the interfacial area density A_i or its flux $A_i v$ account for the dependency on the contact angle (cf. Eq. (16)). The influence of the contact angle on boiling heat transfer is well known. Therefore, it seems reasonable that the boiling heat flux q can be expressed by one the of correlations

$$q = C_1 \Delta T A_i \tag{38}$$

$$q = C_3 \Delta T A_i v \tag{39}$$

where C_2 and C_3 are assumed to be *constant* parameters and ΔT is the superheat. The superheat dependency could also be interpreted by a dependency on the Jakob number $Ja = (\rho_L c \Delta T)/(\Delta h_{\text{vap}} \rho_V)$. Here, ρ_L, ρ_V, c, Δh_{vap} are the liquid and vapor densities, the heat capacity of the liquid, and the latent heat of vaporization, respectively. However, the superheat might not be relevant in the correlations since A_i or $A_i v$ may be self-sufficient measures for the transfer phenomena. However, we will show later, that a better agreement with data is found if we include superheat in the correlation.

7.2. Previously suggested correlations

For transition boiling the most cited empirical model is the one of Berenson [30], who suspected that the transition boiling regime is a combination of nucleate and film boiling. He suggested

$$q = (1 - \alpha_V) q_L + \alpha_V q_V \tag{40}$$

where the boiling heat flux is modelled as a sum of average heat fluxes during liquid and vapor contact, q_L and q_V, respectively, weighted by the area-averaged vapor fraction α_V at the boiling surface. Later many other authors, e.g., [15,31–34] employed this kind of modeling approach who assumed that the average vapor heat flux q_V may be neglected and that the boiling heat flux q_B should correlate with measured $(1 - \alpha_V)$ using an appropriately chosen function for q_L. Many rather empirical functions have been used which were not based on physical insight. Auracher [33] and Nishio and Auracher [34] pointed out that not all relevant parameters have been included in established approaches.

Sadasivan et al. [20] have suggested an energy balance in which they assumed that the three-phase contact line accounts for the entire boiling heat flux due to evaporation. In their critical and fruitful study comparing different mechanisms to the formation of the "macrolayer", they related the density of the contact line to the zeroth moment of the size distribution of the cavities. Recently, Nishio et al. [2] found that the area-averaged line density L_i of the common line (three-phase contact line) at the boiling surface correlates well with high boiling heat flux around critical heat flux (CHF). The common line density was estimated from visual observation of boiling structures on a thin sapphire heater. Thus, they suggested that the heat flux around CHF could be correlated by

$$q = F(\phi) Q_{L,\phi=90^\circ}(\Delta T) L_i \tag{41}$$

where $F(\phi)$ accounts for the influence of the contact angle ϕ on the heat $Q_{L,\phi=90^\circ}$ conducted through a liquid–vapor stem according to the geometry model of Dhir and Liaw [15].

7.3. Discrimination of correlations

The physical significance of the new correlations (38), (39) using interfacial area density or its flux is compared to the previously suggested boiling correlations (40), (41). We could also include correlations employing nucleation site density for their discrimination by utilizing the previously identified nucleation site densities, but delay this to future works, because here the nucleate site density has only been identified up to $\Delta T = 70$ K using a very coarse parameterization of d_S and L.

As discussed in Section 4.2 we have to substitute A_i and $A_i v$ by their approximations given in Eqs. (22) and (26). Thus Eqs. (38), (39) become

$$q = C_1 \Delta T C_1^* f = \widehat{C}_1 \Delta T f \tag{42}$$

$$q = C_3 \Delta T C_3^* f = \widehat{C}_3 \Delta T f \tag{43}$$

Accordingly, if $F(\phi)$ in the correlation (41) is assumed to be a constant C_2, and if the line density is substituted by Eq. (23), and if $Q_{L,\phi=90^\circ} \propto \Delta T$, we obtain

$$q = C_2 \Delta T C_2^* f = \widehat{C}_2 \Delta T f \tag{44}$$

Otherwise, if we assume $F(\phi) = \sin^{-1}\phi$, the correlation of Nishio et al. may also be written as

$$q = Q_{L,\phi=90^\circ}(\Delta T) A_i(\Delta T) \tag{45}$$

replacing line density with interfacial area density using Eq. (16). Then, using the substitutions given in Eq. (22) and assuming that $Q_{L,\phi=90^\circ} \propto \Delta T$ as well as including a constant parameter C_4 again, we get

$$q = C_4 \Delta T C_1^* f \tag{46}$$

By comparing Eqs. (42)–(46), it is obvious that the correlation of Nishio et al. is a somewhat more general correlation and discrimination based on the available single probe data between Nishio's and the new correlation will not be possible. In summary we simply use $C = \widehat{C}_1 = \widehat{C}_2 = \widehat{C}_3 = \widehat{C}_4$ and employ

$$q = C \Delta T f \tag{47}$$

in order to find out if both the correlation of Nishio et al. and the new correlation prove fruitful in correlating boiling heat flux using single probe data.

Therefore, in the following we discriminate the models given in Eqs. (40) and (47).

The solution of the parameter estimation problem

$$\min_{\Theta} \sum_j \left[q_M(\Delta T_j) - q\left(\Theta, \overline{f}_M(\Delta T_j), \overline{\alpha}_{V,M}(\Delta T_j)\right)\right]^2 \tag{48}$$

with q from either Eq. (40) or (47) yields the set of optimal parameters Θ which minimizes the sum of the quadratic difference between the measured boiling curve $q_M(\Delta T_j)$ and the correlated boiling curve $q(\Theta, \overline{f}_M(\Delta T_j), \overline{\alpha}_{V,M}(\Delta T_j))$. $\overline{f}_M(\Delta T_j)$ and $\overline{\alpha}_{V,M}(\Delta T_j)$ are obtained as follows: the contact frequency f_M and vapor fraction $\alpha_{V,M}$ have been measured at eight different superheats and six different wall distances, whereas the boiling curve has been measured at steps of approximately $\Delta T_{j+1} - \Delta T_j = 2$ K [8], because optical probe measurements and heat flux measurements have not been carried out simultaneously. Therefore, optical probe data is linearly interpolated over ΔT to match the superheat resolution of the boiling curve. Since the influence of the spatial dependence of the presence of the interface in the hydrodynamic boundary layer of the boiling process is not yet clear, we employ a spatial average of contact frequency and vapor fraction:

$$\overline{f}_M(\Delta T_j) = \frac{1}{0.99\ \text{mm}} \int_{z=0.01\ \text{mm}}^{z=1\ \text{mm}} f_M(z, \Delta T_j)\,\mathrm{d}z \tag{49}$$

$$\overline{\alpha}_{V,M}(\Delta T_j) = \frac{1}{0.99\ \text{mm}} \int_{z=0.01\ \text{mm}}^{z=1\ \text{mm}} \alpha_{V,M}(z, \Delta T_j)\,\mathrm{d}z \tag{50}$$

Interpolated data for $f_M(z_k, \Delta T_j)$ and $\alpha_{V_M}(z_k, \Delta T_j)$ in steps of $\Delta z_k = 0.01$ mm is employed such that all distances are equally weighted in the integrals.

In order to statistically discriminate the models or combinations of them, the residuals

$$R = \sum_j \left(q_M(\Delta T_j) - q\left(\Theta, \overline{f}_M(\Delta T_j), \overline{\alpha}_{V,M}(\Delta T_j)\right)\right)^2 \tag{51}$$

and the covariance matrix of the parameters V [35] is used. The square roots of the diagonal elements of V, i.e., $\acute{\sigma}_j = \sqrt{V_{j,j}}$, $j = 1, 2, \ldots, p$, represent the standard deviations of each parameter. For model discrimination we compare

$$\sigma_j = \frac{\acute{\sigma}_j}{\Theta_j}, \quad j = 1, 2, \ldots, p \tag{52}$$

for all parameters. The smallest σ_j corresponds to the best parameter estimate and hence to the most correlative model structure.

The residuals and standard deviations for the parameters of the two structurally different models, Eqs. (40) and (47), are summarized in Table 1.

For model equation (47) based on contact frequency (model 1), we have a residual of $R = 102.6$ W·mm^{-2}, whereas for the model equation (40) with vapor and liquid fractions (model 2), an optimal solution is found with a residual of $R = 303.6$ W·mm^{-2}. Although two parameters instead of one have been employed, the residuals of model 2 are nearly three times larger compared to model 1. At the optimal solution the parameter q_L is close to zero and its standard deviation σ_{q_L} is large. Even though in the literature the importance of the term $q_L(1-\alpha_V)$ for transition boiling has been suspected, it can be concluded from this study that $q_L(1-\alpha_V)$ does not correlate well with the boiling curve. Interestingly, $q_V\alpha_V$ correlates quite well as the spatial average of α_V from $z = 0.01$ mm to $z = 1.0$ mm exhibits a relatively similar shape of a typical boiling curve. Since $q_L \approx 0$, the term $q_V\alpha_V$ determines most of the residual of model 2. The single-parameter correlation with contact

Table 1
Estimated parameters, residuals and standard deviations of the parameters for different boiling heat flux models

Model	Eq.	R [W·mm^{-2}]	C [Ws·mm^{-2}·K^{-1}]	q_V [W·mm^{-2}]	q_L [W·mm^{-2}]	σ_C [W·mm^{-2}]	σ_{q_V} [W·mm^{-2}]	σ_{q_L} [W·mm^{-2}]
1	(47)	102.6	0.0037	–	–	0.011	–	–
2	(40)	303.6	–	27.98	1e^{-11}	–	0.038	5.9e^{10}
3	(41), $q_L = 0$	303.6	–	27.98	–	–	0.018	–

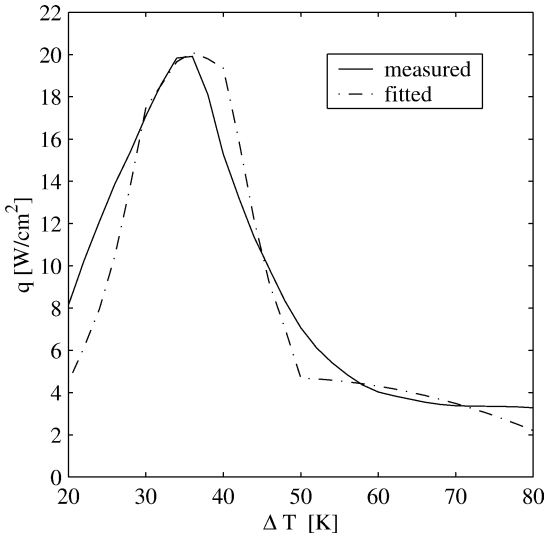

Fig. 10. Measured boiling curve of FC-72 and correlated boiling curve using Eq. (47) with $C = 0.37$ W·cm^{-2}·K^{-1} using data of Hohl et al. [8].

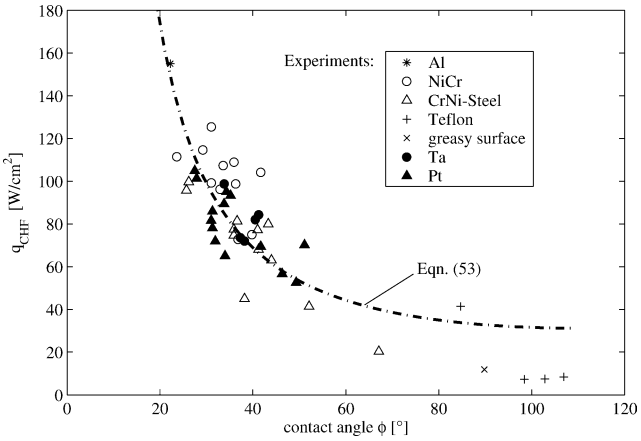

Fig. 11. Influence of contact angle on CHF of boiling water. Experimental data taken from [36] and model prediction according to Eq. (53) with $C_A = 9.6$ W·cm^{-2} and $C_B = 32.8$ W·cm^{-2}.

frequency and superheat leads to an even smaller standard deviation of the fitting parameter C compared to q_V of the two-parameter correlation (model 2, Table 1) as well as of a one-parameter correlation if in Eq. (40) q_L is fixed to zero (model 3, Table 1). The correlated and measured boiling curves are shown in Fig. 10 for the correlation (47) for comparison.

The maximum deviations between the measured and the correlated boiling heat flux are -44% and $+26\%$ which is very good keeping in mind that the entire boiling curve is correlated with a single parameter. Therefore, correlations based on A_i, $A_i v$ or L_i are superior compared to the other proposed correlations and should be subject to further investigations.

If they prove more useful than other correlations then the key to a prediction of boiling heat flux lies in the identification and prediction of the interfacial geometry of the boiling process close to and at the boiling surface and hence proper geometry/interfacial area/contact line density modeling.

7.4. Contact angle and correlating critical heat flux

Unfortunately, we cannot distinguish between $A_i v$, A_i and L_i at the moment. However, we suggest to use interfacial area density or its flux instead of line density for correlating boiling heat flux because of the following reasons: interfacial area density or its flux take into account the direction of the normal unit vector of the interface. This in agreement with Nishio et al. [2] who also pointed out the relevance of the contact angle when correlating boiling heat flux. In Section 3.2 it has been shown that at the boiling surface the normal unit vector on the interface is linked to the contact angle ϕ. Since the contact angle has been found to influence boiling heat transfer to a great extent [12,36], interfacial area density or its flux should better account for this dependence than line density. Secondly, in film boiling the line density at the boiling surface may become zero, but still the presence of interface and its evolution close to the surface has shown to determine local boiling heat transfer by evaporation in film boiling [10]. Therefore, interfacial area density is much closer to the physical and geometrical reality than its alternatives. Mathematically, we have shown (cf. Eq. (16)) that line and interfacial area density for circular structures, e.g., stems, at and close to the boiling surface are on average related by the contact angle. Therefore, in boiling experiments where the contact angle is the only parameter changed while all other parameters are kept constant, i.e., fluid and heater properties, surface roughness as well as vapor fraction and line density at the boiling surface, the change in heat flux due to a change in contact angle should be explainable with interfacial area density. Accordingly, we would expect boiling heat flux to correlate with the result of Eq. (13). Systematic experiments on the CHF of boiling water for different surface wettability conditions measured by the contact angle have been carried out by Hahne et al. [36]. In Fig. 11 their original data is shown together with a least-squares fit of

$$q_{\mathrm{CHF}} = C_A \frac{\tan^{-1}\phi}{\sin\phi} + C_B \frac{1}{\sin\phi} \tag{53}$$

with $C_A = 9.6$ W·cm^{-2} and $C_B = 32.8$ W·cm^{-2}. The constants C_A and C_B have been introduced to retain the structural dependence of the interfacial area density on the contact angle according to Eq. (13) as we lack better information about the particular wetting structure of the considered experiments to fit the CHF data with. Each term in the expressions (13) or (53) contributes a decrease in interfacial area density or heat flux, respectively, with increasing contact angle.

Despite possible uncertainties in the measured CHF due to the employed test heaters in study [36] concerning other influencing factors such as the thermal properties [37], the change of heat flux with contact angle seems to be

qualitatively well correlated with interfacial area density under the given assumptions.

8. Discussion and summary

The interfacial geometry and its evolution close to the boiling surface is shown to be a key factor for a better understanding of the heat transfer phenomena in boiling processes and may be the clue to the development of new mechanistic heat transfer models. A prediction or identification of the interfacial evolution in all its details along the entire boiling curve is currently rather impossible due to the complex nature of the process. Instead, by applying multiphase flow averaging theory we have derived a simple geometry model which connects the size and distance of dry spots, the nucleation site density as well as the contact angle of the wetting fluid with meaningful key quantities of the interfacial geometry such as vapor fraction and interfacial area density in a statistical sense close to the boiling surface. It is revealed that interfacial line and area density are related by the macroscopic contact angle. Subsequently, the model is used to identify the gross features of the interfacial structure of the boiling process from single probe data of the two-phase flow assuming an ergodic process. Good agreement between the volume-averaged model prediction of vapor fraction and interfacial area density and the time-averaged probe data for FC-72 is found. The boiling curve of FC-72 as well as CHF heat flux data of boiling water for different contact angles is successfully correlated with interfacial area density. Discrimination against correlations based on vapor or liquid fraction shows that correlations based on interfacial area density might be superior. We therefore conclude, that the volumetric presence of interface close to the boiling surface plays an important role in the overall heat transfer mechanism. However, due to the use of single optical probe data, some unknowns are left in our approach: the interfacial area density, which we believe is an important quantity for the boiling process, needs to be estimated by the contact frequency measured by the probe using an unknown velocity which was assumed constant along the entire boiling curve. As a consequence this velocity including the contact angle should be measured by multi-tip probes in the future in order to refine the approach presented here. In addition to this, the investigation should be carried out for different fluids and surface materials in order to systematically study the key parameters which have been pointed out in this approach. Obviously, our approach does not allow for a prediction of the boiling curve from fluid and heater data, since the model correlates heat flux with two-phase flow parameters. These quantities are the results of the complex interaction between fluid and heater surface during boiling. Hence, the next major challenge is to correlate these quantities with heater and fluid properties.

Acknowledgements

The authors highly appreciate financial support of Deutsche Forschungsgemeinschaft in the frame of a joint research project on fundamentals of boiling heat transfer. One of the authors, Torsten Lüttich, would like to thank Dr. Drew at Rensellaer Polytechnic Institute very much for fruitful discussions.

References

[1] V.P. Carey, Liquid–Vapor Phase-Change Phenomena, in: Series in Chemical and Mechanical Engineering, Hemisphere, Washington, DC, 1992.
[2] S. Nishio, T. Gotoh, N. Nagai, Observation of boiling structures in high heat-flux boiling, Internat. J. Heat Mass Transfer 41 (1998) 3191–3201.
[3] R.F. Gaertner, Photographic study of nucleate pool boiling on a horizontal surface, J. Heat Transfer 87 (1965) 17–29.
[4] G. Barthau, E. Hahne, Nucleation site density and heat transfer in nucleate pool boiling of refrigerant R134a in a wide pressure range, in: E.W.P. Hahne, W. Heidemann, K. Spindler (Eds.), Proc. 3rd European Thermal-Sciences Conference, Heidelberg, 2000, pp. 731–736.
[5] A. Luke, E. Danger, D. Gorenflo, Size distribution of active and potential nucleation sites in pool boiling, in: J. Taine (Ed.), Proc. 12th Int. Heat Transfer Conf., Grenoble, France, 2002.
[6] D.B.R. Kenning, Experimental methods: Looking closely at bubble nucleation, in: Engineering Foundation Conference Boiling 2000, Alaska, 2000, pp. 1–30.
[7] M. Shoji, A study of steady transition boiling of water: Experimental verification of macrolayer evaporation model, in: Proc. Engineering Foundation Conf. Pool and External Flow Boiling, Santa Barbara, 1992, pp. 237–242.
[8] R. Hohl, H. Auracher, J. Blum, W. Marquardt, Characteristics of liquid–vapor fluctuations in pool boiling at small distances from the heater, in: Proc. 11th Int. Heat Transfer Conference, vol. 2, Kyongju, Korea, 1998, pp. 383–388.
[9] M. Buchholz, T. Lüttich, H. Auracher, W. Marquardt, Experimental investigation of local processes in pool boiling along the entire boiling curve, in: Proc. 5th Int. Conf. Boiling Heat Transfer, May, 2003.
[10] V.K. Dhir, Numerical simulations of pool-boiling heat transfer, AIChE J. 47 (4) (2001) 813–834.
[11] P. Stephan, J. Hammer, A new model for nucleate boiling heat transfer, Wärme- und Stoffübertragung 30 (1994) 119–125.
[12] N. Nagai, V.P. Carey, Assessment of surface wettability and its relation to boiling phenomena, Thermal Sci. Engrg. 10 (3) (2002) 1–9.
[13] P.C. Wayner Jr., Intermolecular forces in phase-change heat transfer: 1998 Kern Award Review, AIChE J. 45 (10) (1999) 2055–2068.
[14] P.C. Wayner Jr., Thermal and mechanical effects in the spreading of a liquid film due to a change in the apparent finite contact angle, J. Heat Transfer 116 (1994) 938–945.
[15] V.K. Dhir, S.P. Liaw, Framework for a unified model for nucleate and transition pool boiling, J. Heat Transfer 111 (1989) 739–746.
[16] J.M. Delhaye, Basic equations for two-phase flow modeling, in: Two-Phase Flow and Heat Transfer in the Power and Process Industries, Hemisphere, Washington, DC, 1981, pp. 40–97.
[17] D.A. Drew, S.L. Passman, Theory of Multicomponent Fluids, Springer, Berlin, 1999.
[18] M. Ishii, Thermo-fluid Dynamic Theory of Two-Phase Flow, Eyrolles, Paris, 1975.
[19] M. Ishii, K. Mishima, Two-fluid model and hydrodynamic constitutive relations, Nuclear Engineering Design 82 (1984) 107–126.
[20] P. Sadasivan, P. Chappidi, C. Unal, R. Nelson, Possible mechanisms of macrolayer formation, Internat. Comm. Heat Mass Transfer 19 (1992) 801–815.

[21] M. Shoji, H. Kuroki, A model of macrolayer formation in pool boiling, in: Proc. 10th Int. Heat Transfer Conference, Brighton, 1994, pp. 147–152.
[22] Y. Katto, S. Yokoya, Principal mechanism of boiling crisis in pool boiling, Internat. J. Heat Mass Transfer 11 (1968) 993–1002.
[23] P. Sadasivan, C. Unal, R. Nelson, Perspective: Issues in CHF modeling—the need for new experiments, ASME J. Heat Transfer 117 (1995) 558–567.
[24] V.P. Carey, On the role of wetting in vaporization and condensation heat transfer, Thermal Sci. Engrg. 10 (6) (2002) 3–9.
[25] L.P. Eisenhart, An Introduction to Differential Geometry, Princeton University Press, Princeton, NJ, 1947.
[26] I. Kataoka, A. Serizawa, Interfacial area concentration in bubbly flow, Nuclear Engrg. Design 120 (1990) 163–180.
[27] D.A. Drew, Evolution of geometric statistics, SIAM J. Appl. Math. 50 (3) (1990) 649–666.
[28] J. Nocedal, S.J. Wright, Numerical Optimization, Springer, Berlin, 1999.
[29] G. Barthau, E. Hahne, Nucleate pool boiling of R134a on a gold-plated copper test tube, in: D. Gorenflo, A. Luke (Eds.), Proc. Int. Refrig. Conf. Comm. B1, Paderborn, October, 2001, pp. 372–379, Session B5.8.
[30] P.J. Berenson, Experiments on pool-boiling heat transfer, Internat. J. Heat Mass Transfer 5 (1962) 985–999.
[31] D.S. Dhuga, R.H.S. Winterton, The pool boiling curve and liquid–solid contact, in: Proc. 8th Int. Heat Transfer Conf., vol. 4, 1986, pp. 2055–2059.
[32] C. Pan, J. Hwang, T. Lin, The mechanism of heat transfer in transition boiling, Internat. J. Heat Mass Transfer 32 (1989) 1337–1349.
[33] H. Auracher, Partielles Filmsieden in Zweiphasenströmungen, Habilitation, Fortschritt-Berichte VDI, Reihe 3, Nr. 142, VDI-Verlag, Düsseldorf, 1987.
[34] S. Nishio, H. Auracher, Film and transition boiling, in: S.G. Kandlikar, M. Shoji, V.K. Dhir (Eds.), Handbook of Phase Change—Boiling and Condensation, Taylor & Francis, London, 1999, pp. 167–196.
[35] Y. Bard, Nonlinear Parameter Estimation, Academic Press, New York, 1974.
[36] E. Hahne, T. Diesselhorst, Hydrodynamic and surface effects on the peak heat flux in pool boiling, in: Proc. 6th Int. Heat Transfer Conference, vol. 1, Toronto, 1978, pp. 209–214.
[37] A. Bar-Cohen, A. McNeil, Parametric effects on pool boiling critical heat flux in dielectric liquids, in: Proc. Engineering Foundation Conf. Pool and External Flow Boiling, Santa Barbara, 1992, pp. 171–175.